

Maltose-Based Fluorinated Surfactants for Membrane-Protein Extraction and Stabilization

Moheddine Wehbie, Kenechi Kanayo Onyia, Florian Mahler, Aline Le Roy, Anaïs Deletraz, Ilham Bouchemal, Carolyn Vargas, Jonathan Oyebamiji Babalola, Cécile Breyton, Christine Ebel, et al.

▶ **To cite this version:**

Moheddine Wehbie, Kenechi Kanayo Onyia, Florian Mahler, Aline Le Roy, Anaïs Deletraz, et al.. Maltose-Based Fluorinated Surfactants for Membrane-Protein Extraction and Stabilization. Langmuir, 2021, 37 (6), pp.2111-2122. 10.1021/acs.langmuir.0c03214 . hal-03162040

HAL Id: hal-03162040

https://hal.univ-grenoble-alpes.fr/hal-03162040

Submitted on 15 Mar 2021

HAL is a multi-disciplinary open access archive for the deposit and dissemination of scientific research documents, whether they are published or not. The documents may come from teaching and research institutions in France or abroad, or from public or private research centers.

L'archive ouverte pluridisciplinaire **HAL**, est destinée au dépôt et à la diffusion de documents scientifiques de niveau recherche, publiés ou non, émanant des établissements d'enseignement et de recherche français ou étrangers, des laboratoires publics ou privés.

Maltose-Based Fluorinated Surfactants for Membrane-Protein Extraction and Stabilization

Moheddine Wehbie,[a] Kenechi Kanayo Onyia,[b,c] Florian Mahler,[b] Aline Le Roy,[d] Anais Deletraz,[a] Ilham Bouchemal,[d] Carolyn Vargas,[b,e,f,g] Jonathan Oyebamiji Babalola,[c] Cécile Breyton,[d] Christine Ebel,[d] Sandro Keller,[b,e,f,g] Grégory Durand[a]*

[a]Institut des Biomolécules Max Mousseron (UMR 5247 UM-CNRS-ENSCM) & Avignon University, Equipe Chimie Bioorganique et Systèmes amphiphiles, 301 rue Baruch de Spinoza – 84916 AVIGNON cedex 9, France;

[b]Molecular Biophysics, Technische Universität Kaiserslautern (TUK), Erwin-Schrödinger-Str. 13, 67663 Kaiserslautern, Germany;

[c]Department of Chemistry, University of Ibadan, 200284 Ibadan, Nigeria;

[d]Univ. Grenoble Alpes, CNRS, CEA, CNRS, IBS, F-38000 Grenoble;

[e]Biophysics, Institute of Molecular Biosciences – IMB, NAWI Graz, University of Graz, Humboldtstr. 50/III, 8010 Graz, Austria;

[f]Field of Excellence BioHealth, University of Graz, Graz, Austria;

[g]BioTechMed-Graz, Graz, Austria.

Corresponding Author. Grégory Durand. E-mail: gregory.durand@univ-avignon.fr ; Phone: +33 (0)4 9014 4445.

Abstract

Two new surfactants, F_5OM and F_5DM, were designed as partially fluorinated analogs of *n*-dodecyl-β-D-maltoside (DDM). The micellization properties and the morphologies of the aggregates formed by the two surfactants in water and phosphate buffer were evaluated by NMR spectroscopy, surface tension measurement (SFT), isothermal titration calorimetry (ITC), dynamic light scattering (DLS), small-angle X-ray scattering (SAXS), and analytical ultracentrifugation (AUC). As expected, the critical micellar concentration (CMC) was found to decrease with chain length of the fluorinated tail from 2.1–2.5 mM for F_5OM to 0.3–0.5 mM for F_5DM, and micellization was mainly entropy-driven at 25°C. Close to their respective CMC, the micelle sizes were similar for both surfactants *i.e.* 7 and 13 nm for F_5OM and F_5DM, respectively and both increased with concentration forming 4 nm diameter rods with maximum dimensions of 50 and 70 nm, respectively, at a surfactant concentration of ~30 mM. The surfactants were found to readily solubilize lipid vesicles and extract membrane proteins (MPs) directly from *Escherichia coli* membranes. They were found more efficient than the commercial fluorinated detergent F_6H_2OM over a broad range of concentrations (1–10 mM) and even better than DDM at low concentrations (1–5 mM). When transferred into the two new surfactants, the thermal stability of the proteins bacteriorhodopsin (bR) and FhuA were higher than in the presence of their solubilization detergents and similar to that in DDM; furthermore, bR was stable over several months. The membrane enzymes SpNOX and BmrA were not as active as in DDM micelles but similarly active as in F_6OM. Together, these findings indicate both extracting and stabilizing properties of the new maltose-based fluorinated surfactants, making them promising tools in MPs applications.

Introduction

Membrane proteins (MPs) are encoded by 20–30% of all genes in most genomes, and they perform a variety of vital functions like solute transport, signal transduction, intercellular recognition and cell adhesion, to name but a few. Moreover, MPs are of great importance since they represent the majority of current drug targets.[1] MPs are usually extracted from native membrane bilayers using a detergent that, ideally, should combine both solubilizing and stabilizing properties so as to preserve the native structures of MPs in non-native environments. Sugar-based surfactants are widely considered mild detergents and have been commonly used as solubilizing and non-denaturing detergents for MP applications including *n*-octyl-β-D-glucoside (OG),[2-3] *n*-decyl-β-D-maltoside (DM),[2] *n*-dodecyl-β-D-maltoside (DDM),[4-6] lactobionamides,[7] and thioglycoside such as *n*-octyl-β-D-thioglucopyranoside (OTG).[8-9] Recently, some sugar-based surfactants with branched polar headgroups or branched hydrophobic tails have been described for the same objective, namely, alkyl diglucosides (DigluM),[10] CALX-173-GK,[11] and laurylmaltose neopentylglycol (LMNG).[12-14] Fluorinated surfactants (FSs) bear several perfluorinated carbon atoms in their hydrophobic tail. The presence of such CF_2 groups makes them more hydrophobic[15] and more surface-active[16-17] than their fully hydrogenated analogues. Moreover, fluorinated chains have a lower affinity for hydrogenated chains, which makes FSs less denaturing towards MPs as they hardly compete with protein–protein and protein–lipid/hydrophobic cofactor interactions.[18] However, earlier neutral FSs were not able to solubilize membrane lipid bilayers, nor extract MPs, rendering classical detergents mandatory for solubilisation, while FSs came into play only at a later stage to stabilize MPs after extraction, when they might already have suffered from irreversible denaturation. Recently, we have demonstrated that fluorination *per se* does not prohibit detergency, with a fluorinated octyl maltoside derivative (F_6OM) showing mild detergency.[19] This nonionic fluorinated surfactant readily interacts with and completely

solubilizes phospholipid vesicles in a manner reminiscent of conventional detergents without, however, compromising membrane order at subsolubilizing concentrations, that is, well below its critical micellar concentration (CMC).

Several series of sugar-based fluorinated surfactants have been synthesized and tested for handling MPs in aqueous solutions. For example, a series of derivatives with various chain lengths, and branched diglucose polar headgroups, showed solubilization of preformed vesicles and efficient extraction of MPs from *E. coli* membranes.[20] Fluorinated analogues of DDM with a maltose polar headgroup were synthesized and found to stabilize the model MP bacteriorhodopsin (bR) over extended periods of time.[21-22] However, to the best of our knowledge, in the literature, none of the earlier sugar-based FSs has been studied for both solubilization and stabilization of MPs.

Currently, however, only a limited number of FSs are available from commercial sources, and their biochemical properties have not been thoroughly investigated. To render FSs more widely accessible and useful, our long-term project is intended to synthesize a range of related compounds in which both head group and tail properties are modified rationally with the aim of tailoring them to the specific needs of MP solubilization, purification, and handling. In this work, we have developed two new maltose-based fluorinated surfactants, called F_5OM and F_5DM, which are analogues of the gold standard DDM (Figure 1). The length of the fluorinated and hydrogenated segments within the hydrophobic chain were chosen in line with our previous observations that the stabilization of the model MP bR is sensitive to the fluorine content,[22] whereas increasing the fluorine content in the hydrophobic chain tends to favor the formation of rod-like large and poorly defined micelles[19] and/or large protein–surfactant complexes.[21] The micellization properties and morphology of aggregates formed by the two surfactants in water were evaluated by NMR spectroscopy, surface tension measurement (SFT), isothermal titration calorimetry (ITC), dynamic light scattering (DLS), small-angle X-

ray scattering (SAXS), and analytical ultracentrifugation (AUC). The efficiency of the synthesized compounds for the extraction and stabilization of MPs were also investigated, on a variety of different MPs: the *E. coli* multidrug transporter, BmrA[23]; a prokaryotic analog of the eukaryotic NADPH oxidases, SpNOX[24]; the *E. coli* outer membrane transporter, FhuA[25]; and bR.[26] The new detergents showed great potency to solubilize lipid vesicles and to extract different proteins from *E. coli* membranes. They also imparted stability to model MPs bR and FhuA, the former protein being still correctly folded after a year of incubation.

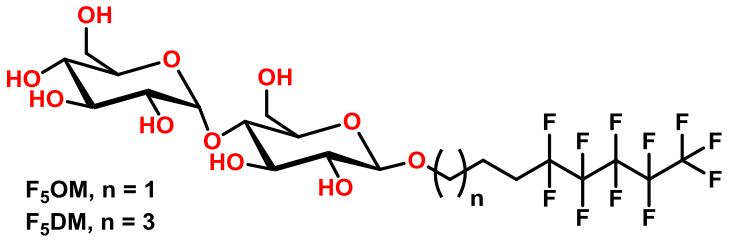


Figure 1. Chemical structures of the new maltoside derivatives.

Experimental Section.

All the fluorinated maltoside derivatives studied in this work are named following the common nomenclature used for their hydrogenated analogs: F_n#M, where n indicates the number of the perfluorinated carbons within the chain starting from the last carbon atom, # indicates the length of the alkyl chain (O for octyl, N for nonyl, D for decyl, UD for undecyl and DD for dodecyl), and M indicates the maltoside polar head. F_5OM indicates the fluorinated analog of octylmaltoside where the last five carbon atoms of the chain are perfluorinated whereas F_5DM indicates the fluorinated analog of decylmaltoside with the last five carbon atoms of the chain being perfluorinated.

All starting materials were commercially available and used without further purification. All solvents were of reagent grade and used as received unless otherwise indicated. CH_3OH was dried over Na under argon atmosphere. CH_2Cl_2 was dried over molecular sieves and stored

under argon. The progress of the reactions was monitored by thin-layer chromatography. The compounds were detected either by exposure to ultraviolet light (254 nm) or by spraying with sulfuric acid (5% ethanol), followed by heating at ~150 °C. ^{1}H, ^{13}C and ^{19}F-NMR analyses were performed at 400, 100 and 376 MHz, respectively. Chemical shifts are given in ppm relative to the solvent residual peak as a heteronuclear reference for ^{1}H and ^{13}C. Abbreviations used for signal patterns are: s, singlet; d, doublet; t, triplet; q, quartet; m, multiplet; dd, doublet of doublet; and dt, doublet of triplet. HRMS (ESI+) was determined on a QStar Elite mass spectrometer. Milli-Q water (resistivity, 18.2 MΩ cm; surface tension, 71.45 mN/m at 25°C) was employed for all physical−chemical experiments.

Synthesis.

Allyl-2,3,6-tri-O-acetyl-4-O-(α-D-2′,3′,4′,6′-tetra-O-acetyl-glucopyranosyl)-β-D-glucopyranoside (2a). Under argon, octa-O-acetyl-ß-D-maltose (3.20 g, 4.71 mmol, 1.0 equiv) was dissolved in dry dichloromethane (10 mL) and the resulting solution was cooled down using an ice bath. Allyl alcohol (0.437 g, 7.54 mmol, 1.6 equiv) was first added followed by the dropwise addition of boron trifluoride diethyl ether complex (0.87 mL, 7.07 mmol, 1.5 equiv). The mixture was stirred at 0 ^{o}C for 2 h and kept at room temperature overnight. Dichloromethane (20 mL) was added, then the mixture was washed with saturated $NaHCO_3$ (2×20 mL) and brine (2×20 mL). The organic phase was collected and dried over anhydrous Na_2SO_4, filtered, and the solvent was removed under reduced pressure. The crude compound was purified by column chromatography on silica gel (cyclohexane/ethyl acetate, 4:6, *v*/*v*) to get **2a** (1.88 g, 59%) as a white powder. R_f (cyclohexane/ethyl acetate, 5:5, *v*/*v*) = 0.28. ^{1}H NMR ($CDCl_3$, 400 MHz): δ/ppm 5.89-5.78 (m, 1H), 5.40 (d, *J* = 3.9 Hz, 1H), 5.35 (t, *J* = 9.4 Hz, 1H), 5.28-5.17 (m, 3H), 5.04 (t, *J* = 9.7, 1H), 4.87-4.82 (m, 2H), 4.57 (d, *J* = 7.9 Hz, 1H), 4.47 (m, 1H), 4.33-4.19 (m, 3H), 4.11-3.93 (m, 4H), 3.67(m, 1H), 2.14 (s, 3H), 2.09 (s, 3H), 2.03 (s, 3H), 2.01 (s, 6H), 1.99 (s, H). ^{13}C NMR ($CDCl_3$, 100 MHz): δ/ppm 170.5,

170.5, 170.2, 169.9, 169.6, 169.4, 133.3, 117.7, 99.0, 95.5, 75.4, 72.7, 72.2, 72.1, 70.0, 69.3, 68.5, 68.0, 62.8, 61.5, 20.9, 20.8, 20.7, 20.6, 20.6, 20.6. HRMS (ESI+) *m*/*z*: $[M+Na]^+$ calculated for $C_{29}H_{40}O_{18}Na$: 699.2112, found 699.2122.

Pent-4-en-1-yl-2,3,6-tri-O-acetyl-4-O-(α-D-2′,3′,4′,6′-tetra-O-acetyl-glucopyranosyl)-β-D-glucopyranoside (2b). 2b was synthesized following the same procedure as for **2a**, from octa-O-acetyl-ß-D-maltose (3.0 g, 4.42 mmol, 1.0 equiv), pentyl alcohol (0.571 g, 6.63 mmol, 1.5 equiv), and boron trifluoride diethyl ether complex (0.82 mL, 6.63 mmol, 1.5 equiv). After purification by column chromatography on silica gel (cyclohexane/ethyl acetate, 3:7, *v*/*v*) compound **2b** (1.16 g, 37%) was obtained as a white powder. R_f (cyclohexane/ethyl acetate, 3:7, *v*/*v*) = 0.21. ^{1}H NMR ($CDCl_3$, 400 MHz): δ/ppm 5.76 (m, 1H). 5.40 (m, 1H), 5.35 (t, *J* = 9.6 Hz, 1H), 5.25 (t, *J* = 9.0 Hz, 1H), 5.09-4.93 (m, 3H), 4.87-4.79 (m, 2H), 4.50 (d, *J* = 7.9, 1H), 4.46 (dd, *J* = 2.6 Hz, *J* = 12.1 Hz, 1H), 4.25 (m, 2H), 4.05-3.93 (m, 3H), 3.85 (m, 1H), 3.66 (m, 1H), 3.48 (m, 1H), 2.13 (s, 3H), 2.09 (s, 3H), 2.06 (m, 2H), 2.04 (s, 3H), 2.01 (s, 6H), 1.99 (s, 6H), 1.62 (m, 2H). ^{13}C NMR ($CDCl_3$, 100 MHz): δ/ppm 170.5, 170.5, 170.3, 170.0, 169.6, 169.4, 137.8, 115.1, 100.3, 95.5, 75.5, 72.8, 72.2, 72.0, 70.0, 69.3, 69.3, 68.5, 68.0, 62.9, 61.5, 29.8, 28.5, 26.9, 20.9, 20.8, 20.7, 20.6, 20.6, 20.5. HRMS (ESI+) *m*/*z*: $[M+H]^+$ calculated for $C_{31}H_{45}O_{18}$: 705.2605, found 705.2600. HRMS (ESI+) *m*/*z*: $[M+Na]^+$ calculated for $C_{31}H_{44}NaO_{18}$: 727.2420, found 727.2393.

4,4,5,5,6,6,7,7,8,8,8-undecafluoro-2-iodo-octyl-2,3,6-tri-O-acetyl-4-O-(α-D-2′,3′,4′,6′-tetra-O-acetyl-glucopyranosyl)-β-D-glucopyranoside (3a). To a solution of **2a** (1.84 g, 2.72 mmol, 1.0 equiv) in dichloromethane (10 mL), perfluoropentyl iodide (0.71 mL, 3.67 mmol, 1.35 equiv) and triethyl borane 1M in hexane (0.5 mL, 0.5 mmol, 0.2 equiv) were added. The mixture was flushed with air and stirred at room temperature for 1 h. 50 mL of a diluted solution of $Na_2S_2O_3$ was added and the aqueous solution was extracted with CH_2Cl_2 (2×50mL). The organic fractions were collected, dried over anhydrous Na_2SO_4, filtered, and

the solvent was removed under reduced pressure. The crude compound was purified by column chromatography on silica gel (cyclohexane/ethyl acetate, 3:7, *v*/*v*) to give compound **3a** (2.51 g, 86 %) as a white powder. R_f (cyclohexane/ethyl acetate, 3:7, *v*/*v*) = 0.24. ^{1}H NMR ($CDCl_3$, 400 MHz): δ/ppm 5.41 (m, 1H), 5.36 (td, *J* = 1.3 Hz, *J* = 10.2 Hz, 1H), 5.26 (td, *J* = 0.8 Hz, *J* = 9.2 Hz, 1H), 5.06 (td, *J* = 2.2 Hz, *J* = 9.9 Hz, 1H), 4.88-4.82 (m, 2H), 4.59 (dd, *J* = 2.5 Hz, *J* = 7.9 Hz, 1H), 4.48 (m, 1H), 4.40-4.17 (m, 3H), 4.11-3.93 (m, 4H), 3.78 (m, 1H), 3.69 (m, 1H), 2.98 (m, 1H), 2.66 (m, 1H), 2.13 (s, 3H), 2.10 (s, 3H), 2.03 (s, 6H), 2.02 (s, 3H), 2.00 (s, 6H). ^{19}F NMR ($CDCl_3$, 376 MHz): δ/ppm –80.7 (td, *J* = 2.7 Hz, *J* = 9.5 Hz, 3F, CF_3), –113.8 (m, 2F, CF_2), –122.6 (m, 2F, CF_2), –123.7 (d, *J* = 52 Hz, 2F, CF_2), –126.3 (t, *J* = 13.6 Hz, 2F, CF_2). ^{13}C NMR ($CDCl_3$, 100 MHz): δ/ppm 170.7, 170.5, 170.3, 170.1, 169.7, 169.7, 169.6, 100.8, 99.8, 95.7, 75.3, 74.9, 73.9, 72.7, 72.5, 71.9, 70.2, 69.5, 68.7, 68.2, 62.7, 61.7, 37.4, 21.0, 20.9, 20.8, 20.8, 20.8, 20.7, 20.6, 13.5. HRMS (ESI+) m/z: $[M+H]^+$ calculated for $C_{34}H_{41}F_{11}IO_{18}$: 1073.1162, found 1073.1156.

4,4,5,5,6,6,7,7,8,8,8-undecafluoro-4-iodo-decyl-2,3,6-tri-O-acetyl-4-O-(α-D-2′,3′,4′,6′-tetra-O-acetyl-glucopyranosyl)-β-D-glucopyranoside (3b). Compound **3b** was synthesized following the same procedure as for **3a**, from **2b** (1.16 g, 1.64 mmol, 1.0 equiv), perfluoropentyliodide (0.88 g, 2.22 mmol, 1.35 equiv) and triethyl borane 1M in hexane (0.3 mL, 0.3 mmol, 0.2 equiv). After purification by column chromatography on silica gel (cyclohexane/ethyl acetate, 2:8, *v*/*v*), compound **3b** (1.70 g, 94 %) was obtained as a white powder. R_f (cyclohexane/ethyl acetate, 3:7, *v*/*v*) = 0.31. ^{1}H NMR ($CDCl_3$, 400 MHz): δ/ppm 5.41 (m, 1H), 5.34 (t, *J* = 10.2 Hz, 1H), 5.23 (t, *J* = 9.2 Hz, 1H), 5.06 (t, *J* = 9.9 Hz, 1H), 4.85-4.76 (m, 2H), 4.50 (d, *J* = 7.9 Hz, 1H), 4.47 (m, 1H), 4.30 (m, 1H), 4.25-4.17 (m, 2H), 4.05-3.94 (m, 3H), 3.85 (m, 1H), 3.65 (m, 1H), 3.52 (m, 1H), 2.80 (m, 2H), 2.12 (s, 3H), 2.08 (s, 3H), 2.02 (s, 3H), 2.00 (s, 3H), 1.98 (2s, 9H), 1.84 (m, 4H).^{19}F NMR ($CDCl_3$, 376 MHz): δ /ppm –80.8 (t, *J* = 9.9 Hz, 3F, CF_3), –111.7 (d, *J* = 270 Hz, 1F, CF_2), –114.7 (d, *J* = 270 Hz,

1F, CF_2), –122.6 (s, 2F, CF_2), –123.9 (t, *J* = 12 Hz, 2F, CF_2), -126.3 (s, 2F, CF_2). ^{13}C-NMR ($CDCl_3$, 100 MHz): δ/ppm 170.5, 170.4, 170.2, 170.0, 169.6, 169.5, 100.1, 95.5, 75.4, 72.7, 72.2, 72.1, 70.0, 69.3, 68.5, 68.0, 62.8, 61.5, 41.6, 36.8, 29.8, 20.9, 20.8, 20.6, 20.6, 20.5, 20.0, 19.8. HRMS (ESI+) m/z: $[M+H]^+$ calculated for $C_{36}H_{45}F_{11}IO_{18}$:1101.1475, found 1101.1476.

4,4,5,5,6,6,7,7,8,8,8-undecafluorooctyl-4-O-(α-D-glucopyranosyl)-β-D-glucopyranoside (4a). Compound **3a** (1.24 g, 1.15 mmol, 1.0 equiv) was dissolved in methanol and 50 mg of Pd/C and sodium acetate (0.310 g, 3.77 mmol, 3.3 equiv) were added portion-wise. The resulting solution was stirred under H_2(g) (6 bars) overnight. The resulting mixture was filtered over a pad of celite and the solvent was evaporated under reduced pressure. The crude product was dissolved in CH_2Cl_2 (50 mL) and washed with a diluted solution of $Na_2S_2O_3$ (50 mL). Then the aqueous phase was extracted with CH_2Cl_2 (2 × 50 mL). The organic fractions were collected, dried over anhydrous Na_2SO_4, filtered, and the solvent was removed under reduced pressure. The resulting compound was dissolved in methanol, then a catalytic amount of sodium methoxide (27 mg, 0.50 mmol) was added portion-wise. The mixture was stirred overnight at room temperature. The reaction mixture was neutralized by addition of Dowex 50W×8-100 ion exchange resin (2.0 g). The ion exchange resin was filtered off and the solvent was removed under reduced pressure. The crude compound was purified by column chromatography on silica gel (CH_2Cl_2/CH_3OH, 85:15, *v*/*v*) to give compound **4a** (0.695g, 91%) as a white powder. R_f (CD_3OD/ethyl acetate, 2:8, *v*/*v*) = 0.27. ^{1}H NMR (CD_3OD, 400 MHz): δ/ppm 5.18 (m, 1H), 4.30 (d, *J* = 7.8 Hz, 1H), 3.98 (m, 1H), 3.94-3.78 (m, 3H), 3.71-3.60 (m, 5H), 3.55 (m, 1H), 3.45 (m, 1H), 3.38 (m, 1H), 3.27 (m, 2H), 2.44-2.25 (m, 2H), 1.92 (m, 2H). ^{19}F NMR (CD_3OD, 376 MHz): δ /ppm –82.5 (td, *J* = 2.7 Hz, *J* = 10.2 Hz, 3F, CF_3), –115.5 (q, *J* = 17 Hz, 2F, CF_2), –123.8 (s, 2F, CF_2), –124.7 (s, 2F, CF_2), –127.5 (s, 2F, CF_2). ^{13}C NMR (CD_3OD, 100 MHz): δ/ppm 104.2, 102.9, 81.3, 77.8, 76.6, 75.1, 74.8, 74.6,

74.2, 71.5, 69.2, 62.8, 62.2, 28.9 (t, *J* = 22.5 Hz), 21.9. HRMS (ESI+) m/z: $[M+H]^+$ calculated for $C_{20}H_{28}F_{11}O_{11}$: 653.1459, found 653.1456.

4,4,5,5,6,6,7,7,8,8,8-undecafluorodecyl-4-O-(α-D-glucopyranosyl)-β-D-glucopyranoside (4b). Compound **4b** was synthesized following the same procedure as for **4a**, from **3b** (1.69 g, 1.54 mmol, 1.0 equiv), 50 mg of Pd/C and sodium acetate (0.404 g, 4.93 mmol, 3.2 equiv) under H_2(g) (6 bars) overnight, followed by deprotection using sodium methoxide (27 mg, 0.50 mmol) to give compound **4b** (0.786 g, 75%) as a white powder. R_f (CD_3OD /ethyl acetate, 2:8, *v*/*v*) = 0.32. ^{1}H NMR (CD_3OD, 400 MHz): δ/ppm 5.16 (d, *J* = 3.8 Hz, 1H), 4.27 (d, *J* = 7.8 Hz, 1H), 3.94-3.78 (m, 4H), 3.71-3.51 (m, 6H), 3.44 (dd, *J* = 3.8 Hz, *J* = 9.6 Hz, 1H), 3.36 (m, 1H), 3.27 (t, *J* = 9.4 Hz, 1H), 3.24 (m, 1H), 2.25-2.0 (m, 2H), 1.65 (m, 4H), 1.53 (m, 2H). ^{19}F NMR (CD_3OD, 376 MHz): δ /ppm -82.5 (td, *J* = 2.3 Hz, *J* = 10.4 Hz, 3F, CF_3), –115.5 (q, *J* = 17 Hz, 2F, CF_2), –123.8 (s, 2F, CF_2), –124.8 (s, 2F, CF_2), –127.5 (s, 2F, CF_2). ^{13}C-NMR (CD_3OD, 100 MHz): δ/ppm 104.3, 102.9, 81.4, 77.9, 76.6, 75.1, 74.8, 74.7, 74.2, 71.5, 70.4, 62.8, 62.2, 31.7 (t, *J* = 22.0 Hz), 30.4, 26.6, 21.1. HRMS (ESI+) m/z: $[M+H]^+$ calculated for $C_{22}H_{32}F_{11}O_{11}$: 681.1769, found 681.1774.

CMC determination by ^{19}F-NMR measurements. Seven samples of each detergent at different concentrations were prepared from stock solutions (4.0 g/L for F_5DM and 6.0 g/L for F_5OM). All samples were dissolved in D_2O/H_2O (10:90, *v*/*v*). CF_3COONa was used as an internal reference (30 μL of a solution at 1 g/L was added). The chemical shifts of the terminal CF_3 group of F_5DM and F_5OM were plotted as a function of the concentration to derive the CMC linear fitting. Below the CMC, the observed chemical shift (δ_{obs}) is the chemical shift of the monomer (δ_{mon}), whereas above the CMC, δ_{obs} is the weighted average of the monomer, and micelle chemical shift, assuming the exchange between the bulk solution and the micelle, is fast on the NMR time scale. If the monomer concentration is constant above the CMC, the observed chemical shift can be written as follows:

$$\delta_{obs} = \delta_{mic} - (\frac{CMC}{C})(\delta_{mic} - \delta_{mon})$$

CMC determination by Surface Tension Measurements. The surface activity of detergents in solution at the air/water interface was determined using a K100 tensiometer (Kruss, Hamburg, Germany). Surface tensions were determined by dilution of stock solutions (0.70 g/L for F_5DM and 5.8 g/L for F_5OM, ~5×CMC) using the Wilhelmy plate technique. In a typical experiment, 20−30 concentration steps were used with ca. 5−10 min between each concentration step. All measurements were performed at (25.0 ± 0.5) °C.

CMC determination by ITC. Demicellization experiments were performed at 25°C on a VP-ITC (Malvern Instruments) by titrating 28 mM F_5OM and 5 mM F_5DM, respectively, from the injection syringe into the sample cell containing triple-distilled water or phosphate buffer. Experimental settings included injection volumes of 5–10 μL, a reference power of 58 μJ/s, a filter period of 2 s, and time spacings of 5 min to allow the signal to reach the baseline before the next injection. Automated baseline adjustment and peak integration were done with NITPIC,[30] and the first injection was always excluded from further analysis. Nonlinear least-

squares fitting was performed in an Excel (Microsoft, Redmond, USA) spreadsheet using the Solver add-in (Frontline Systems, Incline Village, USA), as explained elsewhere.[31]

Analysis of thermodynamic properties. ITC demicellization experiments directly calculates the CMC and the molar enthalpy of micelle formation, $\Delta H_S^{0,\mathrm{aq}\to\mathrm{m}}$. From the CMC, the partition coefficient for micellization, , ${K_S}^{\mathrm{aq}\to\mathrm{m}}$can thus be derived as the ratio of the mole fractions of the surfactant in the micellar (m) and the aqueous (aq) phases: ${K_S}^{\mathrm{aq}\to\mathrm{m}} = X_s^m / X_s^{aq}$. The micellar phase consists only of surfactant molecules, X_s^m=1, whereas $X_s^{aq} = (CMC|C_W + CMC) \approx CMC/55.5\ M$, where C_W denotes the water concentration (55.5 M). From this, the standard molar Gibbs free energy change upon micellization was derived as $\Delta G_S^{0,\mathrm{aq}\to\mathrm{m}} = -RT\ln\left({K_S}^{\mathrm{aq}\to\mathrm{m}}\right) = RT\ln(CMC/55.5\ M)$ and the entropic contribution to micellization as $-T\Delta S_S^{0,\mathrm{aq}\to\mathrm{m}} = \Delta G_S^{0,\mathrm{aq}\to\mathrm{m}} - \Delta H_S^{0,\mathrm{aq}\to\mathrm{m}}$, with $\Delta S_S^{0,\mathrm{aq}\to\mathrm{m}}$ denoting the standard molar entropy change upon micellization.

Dynamic light scattering (DLS). DLS measurements were carried out with a Nano Zetasizer S90 (Malvern, Herrenberg, Germany), utilizing a He–Ne laser at a wavelength of 633 nm as light source and a detection angle of 90°. Samples were transferred to a 45-µL quartz glass cuvette (Hellma, Munich, Germany) and equilibrated for 2 min prior to each measurement. The attenuator was fixed to the maximum position to ensure comparable results for light scattering intensity measurements while in case of the determination of size distributions, attenuator settings were automatically set by the software.

Sedimentation velocity experiments. Sedimentation velocity experiments were performed in a Beckman XL-I analytical ultracentrifuge with a rotor Anti-50 (Beckman Coulter, Palo Alto, USA) and double-sector cells of optical path length 12 mm equipped of Sapphire windows (Nanolytics, Potsdam, DE). Samples were centrifuged at 42000 rpm (130 000 g), at 20°C. Sedimentation velocity profiles were acquired in interference, every 1 min. Data were

analyzed in terms of continuous size distribution c(s) of sedimentation coefficients, s,[27] by using SEDFIT. Peak integration and figures were done with the GUSSI software[28] (http://biophysics.swmed.edu/MBR/software.html). Standard equations and protocols described in [29] were used to derive the refractive index increment, the CMC, the sedimentation coefficient at infinite dilution, s_0. We used the Svedberg equation to derive from s, micelle molar masses, M_{mic}, from which were derived aggregation numbers, N_{agg}, using the information on the calculated surfactant molar masses and partial specific volumes reported on Table 1, and estimates on the hydrodynamic diameters from DLS.

SAXS experiment. Five samples of each detergent at different concentrations were prepared from stock solutions in H_2O (33.3 mM for F_5DM and 29.5 mM for F_5OM). SAXS experiments were conducted on the BM29 beamline at the European Synchrotron Radiation Facility (Grenoble, France). The data were recorded for $0.004<Q<0.5$ Å^{-1} ($Q=(4\pi/\lambda)\sin\theta$ is the modulus of the scattering vector, with 2θ being the scattering angle, and λ the wavelength), using a two-dimensional 1M Pilatus detector, at 20 °C, with a monochromatic X-ray beam with λ = 0.9919 Å and a sample to detector distance of 2.864 m. Measurements were performed with 50 µL loaded sample, in a quartz capillary, with a continuous flow. 10 acquisitions with 0.5 s irradiation (flows of 5 µL/s), were recorded for the samples and water. Data reduction was performed using the automated standard beamline software (BSxCuBE),[30] and data processing, including the elimination of data suffering from radiation damage, averaging, buffer subtraction, Guinier plots, and pair distribution functions, using PRIMUS (V3.1) of the software suite ATSAS.[31] Absolute scales were obtained using the scattering of water. The radii of gyration (Rg) and the intensities scattered in the forward direction (I(0)) were extracted by the Guinier approximation, with RgQ ≤ 1.0. The molar mass of the micelle, M_{mic}, was derived from $M_{mic} = (I(0)/c_{mic})N_A/(\partial\rho_{el}/\partial c)^2$, with N_A Avogadro's number, c_{mic} the micelle concentration (g mL^{-1}), calculated using the CMC-values from ITC, and $\partial\rho_{el}/\partial c$ (cm

g^{-1}) given in table S#1. the increment of electron scattering length density per g of surfactant. Aggregation numbers N_{agg} were then derived from M_{mic}. The maximum dimensions (D_{max}) were estimated from the pair distribution functions. Shape analysis were done using shape-dependent models in SASview (V4.2.1) (https://www.sasview.org/). We investigated the cylinder models. Theoretical SLD values are given in table S1. The form factor included size polydispersity on radius (fixed at 15 %, this value resulting from preliminary fits) using a gaussian distribution. The scale factor (i.e. the surfactant concentration in vol/vol unit), and the SLD of the solvent were constrained (table S1). The core radius and cylinder length were adjusted. Note that for F_5DM scattering curves, we also performed an analysis with core shell cylinder model. The scale factors, the core and solvent SLDs were fixed (table S1) and core radius, thickness and SLD shell, and cylinder length were adjusted. The two fits in the cylinder and core shell cylinder models were equivalent in terms of quality, as evaluated by the chi2 values. But the later provided inconsistent values for the lowest concentrations; for the three largest concentrations, the radius and the thickness were constant: 1.79 ± 0.09 and 1.16 ± 0.1 nm, respectively, thus the sum (radius + thickness) was rather large (2.95 nm). The mean value of the fitted SLD shell (1.07 ± 0.02 10^{-5} $Å^{-2}$) corresponded to 75 % water. The very large dimension of the total radius associated to overestimated hydration in the core-shell cylinder model can be due to the fact that the SLDs of the anhydrous head and tail are rather close (1.51 10^{-5} $Å^{-2}$ and 1.44 10^{-5} $Å^{-2}$) compared to water (9.53 10^{-6} $Å^{-2}$), which argues in favor of the simple cylinder model.

Preparation of lipid vesicles. To prepare LUVs, POPC in powder form was weighed on a high-precision XP Delta Range microbalance (Mettler Toledo, Greifensee, Switzerland) and suspended in phosphate buffer (10 mM Na_2HPO_4/NaH_2PO_4, 150 mM NaCl, pH 7.4). The solution was vortexed for 15 min at room temperature and extruded in a LiposoFast extruder (Avestin, Mannheim, Germany) with at least 35 extrusion steps through two stacked

polycarbonate membranes with a pore diameter of 100 nm (Avestin). The hydrodynamic diameter of the LUVs was distributed around 120–130 nm, as shown by DLS.

Kinetics of vesicle solubilization. For vesicle solubilization kinetics, measurements were conducted by adding a high concentration (5 mM) of the respective surfactant above its CMC to 100 μM POPC LUVs in a 3 mm×3 mm quartz glass cuvette. Measurements were started immediately after mixing the vesicle suspension to monitor changes in light scattering intensity, $I_{scatter}$.

Solubilization of MPs from native *E. coli* membranes. *E. coli* BL21(DE3) cells were transformed with an empty pET-24 vector and selected by kanamycin resistance. After incubation in 400 mL lysogeny broth overnight at 37°C under constant agitation (150 rpm), cells were harvested by centrifugation and washed twice with saline (154 mM NaCl). Cell pellets were resuspended in ice-cold buffer (100 mM Na_2CO_3, pH 11.5) and subjected to ultrasonication in an S-250A sonifier (Branson Ultrasonics, Danbury, USA) twice for 10 min each. To remove cell debris, the lysate was centrifuged at 4°C for 20 min at 3000 *g*. The supernatant was ultracentrifuged at 4°C for 1 h at 100,000 *g* to separate membrane fragments from soluble and peripheral proteins. Membrane pellets were washed and suspended in working buffer, ultracentrifuged again at 4°C for 1 h at 100,000 *g* to remove any residual soluble or peripheral proteins. The resulting pellets were resuspended in buffer (50 mM Tris, 200 mM NaCl, pH 7.4) to a final concentration of 100 mg wet-weight pellet per 1 mL of buffer and mixed in a 1:1 volume ratio with stock solutions of DDM or FSs in buffer. Surfactant concentrations were chosen on the basis of the CMC values determined in this study to ensure comparable extraction conditions. All samples were incubated for at least 16 h at 20°C under constant, gentle agitation (500 rpm) and subsequently ultracentrifuged at 4°C for 1 h at 100,000 *g*. The solubilized supernatant containing micelles was analyzed using SDS-PAGE.

Sodium dodecyl sulphate polyacrylamide gel electrophoresis (SDS-PAGE). The solubilization efficiency of the two FSs on biological membranes was assessed by SDS-PAGE using a NuPAGE Bis–Tris system (Life Technologies, Carlsbad, USA) with a polyacrylamide gradient of 4–12%. 14-µL samples were mixed with 5 µL 4x SDS sample buffer (106 mM Tris HCl, 141 mM Tris base, 2% (*w/v*) SDS, 10% (*w/v*) glycerol, 0.51 mM EDTA, 0.22 mM SERVA Blue G250, and 0.175 mM Phenol Red, pH 8.5) and 1 µL 1 M dithiothreitol (DTT) and boiled at 95°C for 10 min. 12 µL of each sample was loaded on a ready-to-use NuPAGE. As reference, a standard-weight marker (Roti-Mark 10–150, Carl Roth, Karlsruhe, Germany) was used, and the working buffer was used as negative control. Gel electrophoresis was performed for 45 min in MES buffer (50 mM MES, 50 mM Tris base, 0.1% (*w/v*) SDS, 1 mM EDTA) at 200 V and 50 W. Subsequently, gels were fixed for 20 min (10% (*w/v*) acetic acid, 40% (*w/v*) ethanol), stained for 30 min (0.025% (*w/v*) Coomassie brilliant blue G250, 10% (*w/v*) acetic acid) and destained overnight in water. For quantification of solubilization efficiencies, gels were photographed with a C4000Z camera (Olympus, Tokyo, Japan), and protein bands were analyzed with ImageJ.[32]

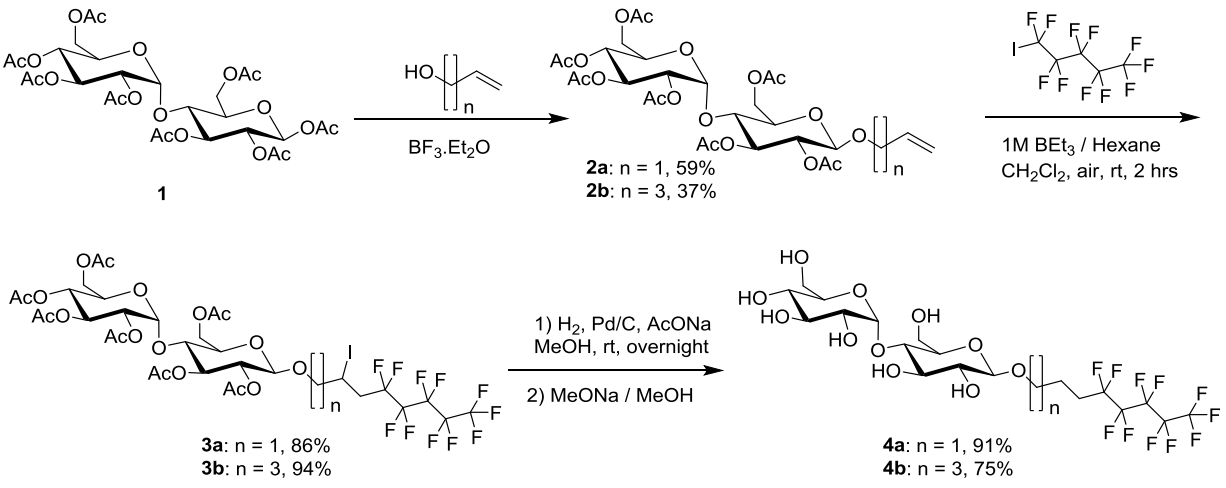
Thermal denaturation assays. Thermal unfolding analysis were performed by differential scanning fluorimetry coupled to back scattering using a Prometheus NT.48 instrument (Nanotemper Technologies, Munich, DE), and the provided software PR.thermocontrol v2.0.4. Up to 48 capillary containing 10 µL of sample are sequentially illuminated at 280 nm, and fluorescence intensity at 350 (F350) and 330 (F330) nm, and back scattering measured as a function of temperature. The temperature was increased by 1 °C/min from 15 °C up to 90 or 95°C °C. The derivatives of F350/F330 and of the back scattering were used to estimate the melting temperature, T_m, and the onset of aggregation, T_{agg}, respectively. FhuA and bR samples are described in Breyton et al.[12]

bR solubilization and detergent exchange by sucrose gradient. Sucrose gradients are a convenient means to perform both detergent exchange and evaluate the colloidal homogeneity of the protein-detergent complex. We routinely use this method to evaluate the potentialities of fluorinated surfactants in the biochemistry of MPs.[32] BR retinal molecule, whose visible absorption spectrum is very sensitive to its local environment, is a convenient reporter of the state of the protein: the trimeric protein in its native membrane reveals a visible absorption spectrum with a maximum at λ_{max} = 570 nm; when solubilized in detergent, the protein monomerizes and displays λ_{max} ~ 550 nm; the protein appears purple/pink. When the protein denatures, the retinal is released, and λ_{max} shifts to 400–380 nm: the protein solution turns yellow. We have reported that when the solubilized monomeric protein is transferred into a fluorinated surfactant, fluorinated surfactant migrates deeper in the gradients, due to the higher density of the surfactant, and λ_{max} can shift to ~ 610 nm, giving a blue color to the protein-surfactant complex.[32] Diffusion of the absorption curve is a witness of the appearance of larger particles in the solution, suggesting either aggregation of the protein or the formation of membrane patches.

Purified purple membrane was solubilized for 40 h at 4°C with 89mM OTG (CMC = 9 mM) at a membrane concentration of 1.5 g L^{-1} in 20mM sodium phosphate buffer, pH 6.8. Samples were diluted to reach a final OTG concentration of 15 mM, supplemented with 2 mM of the surfactant to be tested, and incubated 15 min prior to being loaded onto a 10–30% (w/w) sucrose gradient containing 20 mM sodium phosphate buffer pH 6.8 and 6 mM of either DDM as a control, or the surfactant to be tested. Gradients were centrifuged for 5 h at 55,000 rpm (200,000 *g*) in the TLS55 rotor of a TL100 ultracentrifuge (Beckman). Bands containing the colored protein were collected with a syringe, and protein samples were kept at 4°C in the dark for UV–visible spectrophotometry.

Results and Discussion.

Synthesis. The detergents were synthesized in four steps, as illustrated in Scheme 1. The synthetic route is inspired by that previously used for the preparation of the poorly fluorinated analog of undecylmaltoside with two perfluorinated carbons F_2UDM (also called F_2H_9Malt).[22] Compounds **2a** and **2b** were prepared starting from peracetylated maltose by glycosylation reaction with allyl alcohol and penten-1-yl alcohol, respectively. The double bonds of the obtained compounds (**2a** and **2b**) were then subjected to free radical reaction with perfluoropentyl iodide in the presence of 1 M BEt_3 in hexane.[33] The addition of the fluoroalkyl chain to the double bonds was confirmed by ^{1}H- and ^{13}C-NMR, which showed the disappearance of the signals corresponding to the double bond and the formation of new signals of -CHI. The iodine group of compounds **3a** and **3b** was reduced under H_2 gas and in the presence of Pd/C as catalyst. The obtained compounds were then deprotected under Zemplén conditions,[34] using a catalytic amount of MeONa in MeOH to obtain the desired detergents **4a** and **4b**. The crude detergents were purified by chromatography and freeze–dried to give the pure detergents in satisfactory global yields of 46% and 26% for F_5OM and F_5DM, respectively.



Scheme 1. Synthesis of F_5OM (**4a**) and F_5DM (**4b**).

Micellization. Micellization of the two surfactants was characterized by means of ITC, ^{19}F-NMR, and SFT, from which we derived micellar parameters (Table 1). The critical micelle concentration (CMC) values were in very good agreement among the three techniques (Figure 2 and Figure S1). While F_5OM exhibited a CMC around 2.3 mM, the longer-chain derivative F_5DM had a CMC of ~0.4 mM. Thus, addition of two more methylene groups to the chain led to a decrease in CMC by a factor of ~5, which is only half the effect predicted by Traube's rule[35] for adding two methylene groups to an alkyl chain.

The changes in Gibbs free energy $\Delta G_S^{\mathrm{m/aq},^\circ}$, enthalpy $\Delta G_S^{\mathrm{m/aq},^\circ}$, and entropy $-T\Delta S_S^{\mathrm{m/aq},^\circ}$, accompanying the transfer of surfactant monomers from the aqueous solution into micelles are also summarized in Table 1. These data showed that micellization was almost exclusively driven by entropy, with enthalpy making only a minor contribution that decreased with increasing chain length. The Gibbs free energy of micellization increased in magnitude by –4.2 kJ/mol upon increasing the chain length by two CH_2 groups. In addition, the fluorinated maltoside-based surfactants displayed a higher tendency to form micelles at lower concentration than their hydrogenated analogues bearing the same number of carbon atoms in their hydrogenated chains. The hydrophobic contribution to micelle formation, that is, the contribution of the alkyl tail of F_5DM (CMC = 0.39 mM), which contains 10 carbon atoms, was greater than that of its decyl hydrogenated analogue DM (CMC = 2.0 mM) and fall between that of the undecyl derivative UDM (CMC = 0.59 mM) and DDM (CMC = 0.17 mM).[36] Similarly, the alkyl tail of F_5OM (CMC = 2.21 mM), which contains 8 carbon atoms, had almost similar hydrophobic contribution as DM. The hydrophobic contribution of CF_2 in highly fluorinated surfactants follows the rule that 1.0 CF_2 moiety has about the same effect as 1.5 CH_2 moieties;[37] hence, the CMC of F_6OM (0.71 mM) is similar to that of UDM (0.59 mM). This is once again confirmed with the two F_5DM and F_5OM where $1CF_2$ = 1.3-1.6×CH_2. By contrast, sparingly fluorinated FSs do not obey this rule. Indeed, it has been

observed that the hydrophobic contribution of a CF_2 unit depends on the length of the fluorinated tip at the end of the aliphatic chain.[37] For instance F_2H_9Malt,[22] the fluorinated analog of UDM with two perfluorinated carbons (F_2UDM following our nomenclature) has a CMC of 1.14 mM which is close to that of DM (1.8 mM) and would correspond to $1CF_2 = 0.5\times CH_2$.

SFT data were used to construct Gibbs adsorption isotherms (data not shown) to determine the surface excess concentration at surface saturation, Γ_{max}. The values observed for F_5OM (2.79×10^{-12} mol/mm^2) and F_5DM (2.87×10^{-12} mol/mm^2), thus indicate similar packing of the two detergents at the air/water interface. From these values, the areas occupied per detergent molecule at the air/water interface, A_{min}, were determined to be close to 60 Å^2 for both compounds.

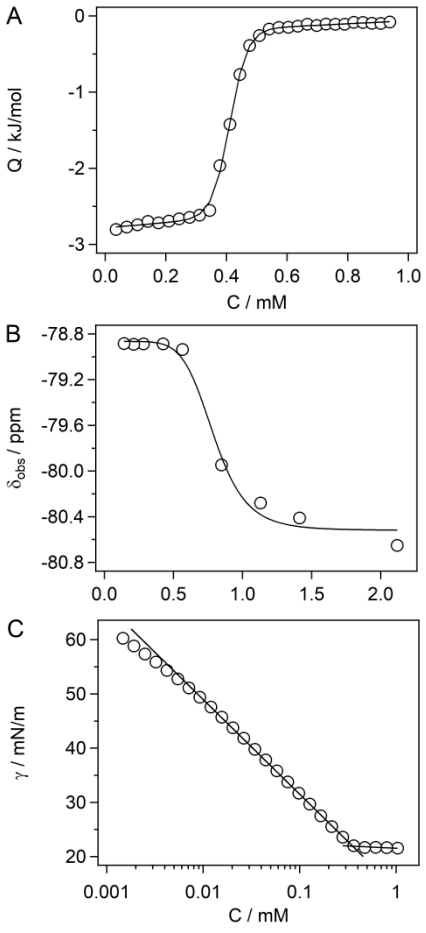


Figure 2. (A) ITC data for F_5DM. Shown are an experimental isotherm (*open symbols*) and a fit based on a generic sigmoidal function (*solid line*). (B) ^{19}F NMR peak chemical shift, δ_{obs},

versus F_5DM concentration. We followed the signal of the terminal CF_3 group of the chain. The solid line represents the nonlinear fit of the experimental points.[38] (C) Surface tension versus F_5DM concentration. The solid lines represent the linear fit of the experimental points and the intersection corresponds to the CMC.

Size and shape of the micelles. We next investigated the self-assembly properties of the FSs in phosphate buffer using DLS. At 10 mM, volume-weighted particle size distributions for F_5OM and F_5DM revealed unimodal distributions of rather small micelles with hydrodynamic diameters ranging from ~8 nm for F_5OM to ~15 nm for F_5DM (Figure 3A). Upon dilution to 5 mM, no significant difference in the volume-weighted distributions was observed for both compounds yet with a small decrease of the hydrodynamic diameters to ~7 nm for F_5OM and to ~13 nm for F_5DM (data not shown).

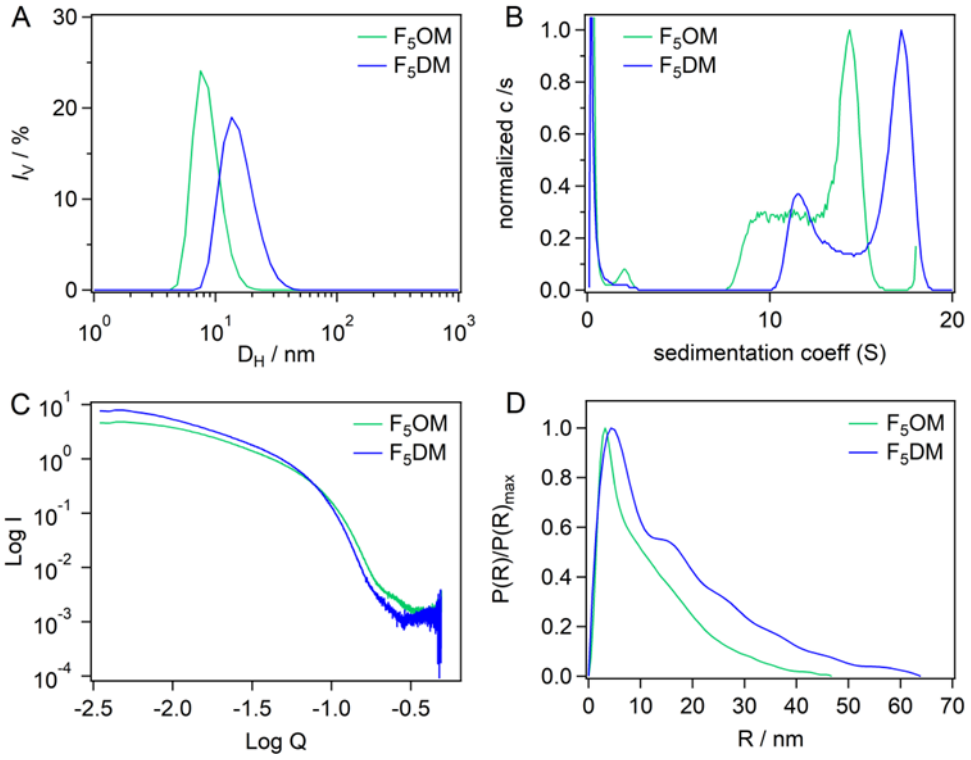


Figure 3. (A) Volume-weighted particle size distributions for F_5OM and F_5DM at 10 mM in phosphate buffer. (B) Distributions of sedimentation, *c*(s), for F_5OM at 10.5 mM and F_5DM at 7.7 mM. (C) SAXS patterns, and (D) pair distribution functions for F_5OM at 23.6 mM and F_5DM at 24.6 mM.

Table 1. Micellar Properties of Maltose Derivatives.

Detergent		**F_5OM**	**F_5DM**
Molecular Weight g/mol		652	680
ITC[a]	CMC (mM)	2.21 ± 0.07	0.39 ± 0.01
	$-T\Delta S°_{mic}$ (kJ/mol)[b]	–28.53 ± 0.53	–32.01 ± 0.04
	$\Delta H°_{mic}$ (kJ/mol)[c]	3.43 ± 0.46	2.57 ± 0.20
	$\Delta G°_{mic}$ (kJ/mol)[d]	–25.10 ± 0.08	–29.43 ± 0.04
	K^{mic}	$2.5\times10^4 \pm 0.08\times10^4$	$14.5\times10^4 \pm 0.23\times10^4$
NMR[*]	CMC (mM)	2.67	0.53
ST[a]	CMC (mM)	2.13 ± 0.10	0.34 ± 0.02
	γCMC (mN/m)[e]	20.6	21.7
	$\Delta G°_{mic}$ (kJ/mol)[d]	-25.2 ± 0.1	-29.7± 0.1
	Γ_{max} (10^{-12} mol/mm^2)	2.79 ± 0.01	2.87 ± 0.13
	A_{min} (Å²)[f]	59.6 ± 0.2	58.0 ± 2.6
DLS	D_H (nm)[g] at 5 mM	7.4	12.8
	D_H (nm)[g] at 10 mM	8.3	14.8
AUC-SV	$\bar{v}$ (mL/g)	0.571	0.595
	$\partial n/\partial c$ (mL/g)	0.064	0.074
	CMC (mM)[h]	2.5	0.3
	s_0 (S)[i]	12.1 ± 0.2	11.1 ± 0.2
	s (S) at CMC + 5 mM[i]	12.7 ± 0.2	14.1 ± 0.2
	k's (mL/g)[j]	9 ± 4	77 ± 12
	N_{agg} at CMC + 5 mM [k]	200	380
SAXS	C-CMC range (mM)	1.8 - 31	2.5 - 29
	Rg (nm) range[l]	6.5 - 10	5.8 – 13.5
	N_{agg} range[l]	270 - 335	300 - 500
	D_{max} (nm) range[m]	27 - 50	30 -70
	Fitted SLD (Å^{-2})[n]	13.8 ± 0.7	12.8 ± 0.4
	Hydration (g water /g surfactant)[n]	0.18 ± 0.12	0.34 ± 0.11
	Radius (nm)[n]	1.95 ± 0.03	2.25 ± 0.03
	Length (nm) range[n]	18 - 30	14 - 38

[a]Data are averages of at least two experiments unless noted by * for one experiment only. ± indicates 95% confidence interval boundaries from a nonlinear least-squares fit for ITC. ± indicates standard errors from at least two experiments for SFT, AUC and SAXS. [b]Entropic contribution to micelle formation. [c]Enthalpic contribution to micelle formation. [d]Gibbs free energy of micellization. [e]Surface tension attained at the CMC. [f]The surface excess (Γ_{max}) and the surface area per molecule (Å²) were estimated from the slope of the surface tension curve. [g]Hydrodynamic diameter by volume in phosphate buffer. [i]Sedimentation coefficient at infinite dilution (s_0), or linearly interpolated from experimental data at CMC+ 5 mM, in water at 20 °C. [j]Concentration dependence factor k's from linear fits. [k]Aggregation number obtained from s, and D_H. Error is estimated at 10%. [l]radius of gyration and aggregation numbers from Guinier analysis. [m]Maximum distance from $P(R)$ analysis. [n]Fitted scattering length density, derived hydration, radius and length considering a cylinder model.

To further characterize the micellar aggregates, AUC sedimentation velocity experiments were performed. Figure S2A displays the sedimentation velocity profiles. From the $c(s)$ analysis, we observed a complex boundary representing micelles in the range 9-16 S for

F_5OM and 10-18 S for F_5DM (Figures 3B, S2B and S2B'). The *s* value increased with concentration, with a more pronounced effect for F_5DM than for F_5OM (Figure S2D). We used the dilution series to determine, from the micelle signals versus concentration, the refractive index increment ($\partial n/\partial c$) and the CMC, as well as the *s* value at infinite dilution (s_0) and the concentration dependence factor (*k*'s) (Figure S2C and Table 1). For both detergents, AUC provided CMC values relatively similar to those–obtained from NMR, SFT, and ITC (Table 1). The s_0 values are similar, but sedimentation coefficients vary with concentration to different extents for the two surfactants as illustrated by the k'$_s$ values. A realistic estimate of aggregation numbers, N_{agg}, is obtained by combining the values of *s* with that of the hydrodynamic diameters from DLS. Calculated N_{agg} at the CMC+5mM are lower for F_5OM compared to F_5DM (Table 1).

To complete the colloidal characterization of the two compounds, SAXS experiments were next performed. Figure 3C shows the scattering curves for F_5OM and F_5DM whose similarities in the shape suggest similar micelle organization (See Figure S3 for detailed analysis). Guinier analysis at low angle (Figure S3B) provided mean radius of gyration (Rg) and N_{agg}, which increase with concentrations, moderately for F_5OM and to a larger extent for F_5DM (Table 1 and Figure S4). Pair distribution functions, $P(R)$, derived from the whole scattering curves (Figure 3D and S3C) present for F_5OM a main maximum at 3.5 nm which remains invariant while it increases slightly with concentration for F_5DM from 3.6 to 4.6 nm. All curves present at larger *R* a linear decrease, which indicates a linear rod shape for the aggregates.[39] The largest distance, D_{max}, corresponding to $P(R)$ reaching zero, increases with concentration for both surfactants, and in minor extent for F_5OM compared to F_5DM (from ≈ 30 for both to 30 and 50 nm, respectively). Lastly, we analyzed the scattering curves considering a cylinder with hard sphere interaction. The fitted and experimental curves are reasonably superposed for all scattering curves (Figure S3D). Table S2 presents the detailed

results, and Table 1 reports the main conclusions. The values of the fitted scattering length density (SLD) do not depend on surfactant concentration, as expected, and are intermediate between anhydrous surfactant and water SLDs. We derived reasonable hydration of 0.18 ± 0.12 and 0.34 ± 0.11 g of water per g of surfactant. Fitted radius do not vary with surfactant concentration: 1.95 and 2.25 nm for F_5OM and F_5DM, respectively. It is comparable to the sum, determined from SAXS and SANS, of the core radius and shell thickness, for the small dimension (≈ 2.1 nm) of the slightly elongated DDM micelle,[12, 40-41] or for the lateral dimension (2.2 nm) of the rod-forming detergent LMNG, which also bears maltose heads and have two dodecyl chains.[12] Because the fitted SLD and radius-values are correlated with the concentration input values, the minor differences in the fitted hydration and radius for the two surfactants may be irrelevant. The length is ≈ 15 nm at the lowest concentrations, and reaches 30 and 38 nm at ≈ 30 mM F_5OM and F_5DM, respectively (Figure S3D). These values correspond to length/diameter ratio of ≈ 8. We note that the fitted length is about half D_{max}. A tentative explanation is that there is a distribution in length. D_{max} probes the largest molecules, while the fit considers the most populated dimensions.

The larger micelle size above 5mM, for F_5DM versus F_5OM observed from AUC and SAXS is in line with what is generally observed for hydrogenated[42] and fluorinated detergents.[20] Comparing with fluorinated compounds with the same OM head-group, while the hydrogenated DDM forms small slightly elongated micelles of ≈60 kDa up to at least 10 mM [29], the poorly fluorinated F_2UDM and the nonyl derivative with four perfluorinated carbons F_4NM (also called F_4H_5Malt)[22]were described to form small micelles with N_{agg} < 100 up to C-CMC ≈ 10 mM (*s* of 4 and 7 S at CMC + 5 mM), the later experiencing very slightly attractive interactions evidenced only above 30 mM. The commercial F_6OM forms very large rod micelles with N_{agg} > 500 at ≈ CMC + 10 mM (*s* of 27 S at CMC + 5 mM). The propensity of highly fluorinated surfactants with a OM head to form rather large rods is in contrast with

fluorinated surfactants with a head bearing two glucose groups, which self-assemble into compact and well-defined globular micelles of 6–8 nm in diameter with aggregation numbers below 100.[20]

Solubilization of POPC LUVs by FSs. The detergency reflects the ability of an amphiphilic compound to both solubilize lipid bilayers and extract MPs. To assess the detergency of F_5OM and F_5DM, we tested whether they are able to dissolve large unilamellar vesicles (LUVs) composed of the singly unsaturated phospholipid 1-palmitoyl-2-oleyl-*sn*-glycero-3-phosphocholine (POPC). Measurements were conducted at 25°C by adding a rather high concentration (CMC+5 mM) of the respective FS to 100 μM POPC LUVs, which resulted in a steady decrease in the light scattering intensity over time. The particle size distributions shown in Figure 4 support the interpretation that the decreased light scattering intensity was due to vesicle solubilization, as the vesicular peak at ∼120 nm at the beginning of the measurement completely disappeared after the intensity decreased to the level of pure mixed micelles. Solubilization was essentially complete after ∼16 h for F_5DM but took longer for F_5OM. Most importantly, however, both FSs were able to solubilize synthetic POPC vesicles at 25°C, which sets them apart from more conventional FSs such as F_6OM, F_4H_2-DigluM, F_6H_2-DigluM, and F_8H_2-DigluM, which require elevated temperatures and prolonged incubation times for solubilization.[19-20]

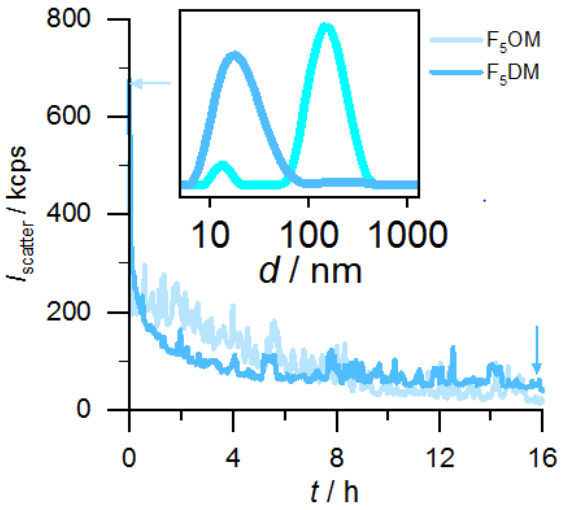


Figure 4. Kinetics of 100 µM POPC LUVs solubilization by 7.2 mM F_5OM & 5.4 mM F_5DM at 25°C as monitored in terms of the light scattering intensity recorded at an angle of 90°. The inset shows intensity-weighted size distributions obtained for a mixture of 100 µM POPC and F_5DM immediately (green) or after 16h (blue). Buffer: 10 mM phosphate, 150 mM NaCl, pH 7.4.

Extraction of MPs from native *E. coli* membranes. Next, we investigated whether F_5OM and F_5DM can also extract MPs from native *E. coli* membranes. To this end, we quantified the intensities *(i.e.*, pixel counts) of SDS-PAGE band patterns (Figure 5A) and compared their efficiencies with those of DDM and F_6OM. The overall protein-extraction yields were also expressed relative to the buffer without any detergent (Figure 5B). Figure 5A indicates that both F_5OM and F_5DM extracted similar patterns of MPs spanning a broad size range. Notably, at low concentrations (*i.e.*, 1–5 mM), both FSs displayed better solubilization efficiencies than DDM, although DDM was outstanding in extracting a single abundant protein of ~35 kDa, namely, outer-membrane protein OmpA, at higher concentrations. By contrast F_6OM showed very limited solubilization.

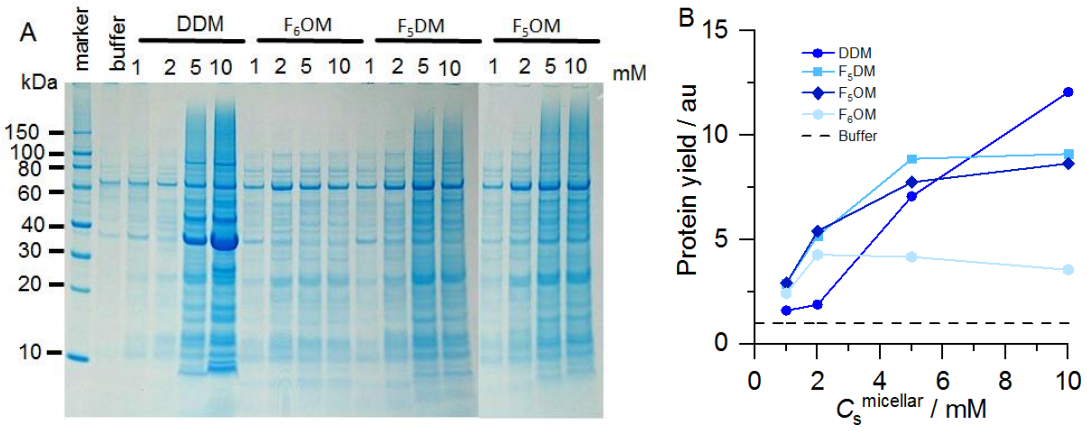


Figure 5. (A) SDS-PAGE of *E. coli* membrane extracts upon exposure to various FSs with micellar concentrations as indicated. (B) Graphical representation of *protein*-extraction yields (symbols) when using surfactant relative to the yield obtained when no surfactant was added (i.e., only buffer; *dashed line*). Data are mean values from three experiments.

FhuA and bR thermal stability. To assess the stability of MPs in the new FSs, we investigated the thermal stability of two models proteins. Differential scanning fluorimetry (DSF) probes conformation changes with temperature. It allows measuring the melting temperature (T_m) of the protein by measuring the fluorescence emission (F_{350nm}/F_{330nm} ratio) of the aromatic residues upon increasing temperature. Simultaneous light back-reflection measurement probes protein aggregation, T_{agg} being the onset temperature for aggregation. FhuA is an *E. coli* outer membrane ferrichrome-iron transporter involved in bacteriophage infection.[43] bR is a light-driven proton pump purified from the archaea *Halobacterium*. It binds a covalent cofactor, a retinal molecule that confers a purple color to the protein.[44] We use the two proteins, representatives of the two main structural classes ß-barrels and α-helix bundle, of proteins, to investigate their thermal stabilities in the presence of our fluorinated derivatives. The two proteins were first extracted by lauryldimethylamine oxide (LDAO) for FhuA and OTG for bR, and then transferred into F_5OM and F_5DM, as well as in DDM and the solubilizing detergent, at CMC + 0.2 mM, and CMC + 2 mM. Final residual concentrations of the initial detergents, LDAO for FhuA and OTG for bR, were 0.05 and 0.4 CMC. FhuA shows two unfolding events (Figure 6), attributed to, first, the unfolding of the cork, at T_{m1},

and then of the barrel, at T_{m2},[45] while bR shows only one transition (Figure S5). For each of the two proteins, the melting curves general appearance is similar whatever the detergent and its concentration. Table 2 presents the mean values of T_m and T_{agg}. For FhuA and bR, in LDAO or OTG the extracting detergents, T_m are lower than that in F_5OM, F_5DM or DDM suggesting a thermostabilizing effect of the three maltoside derivatives.

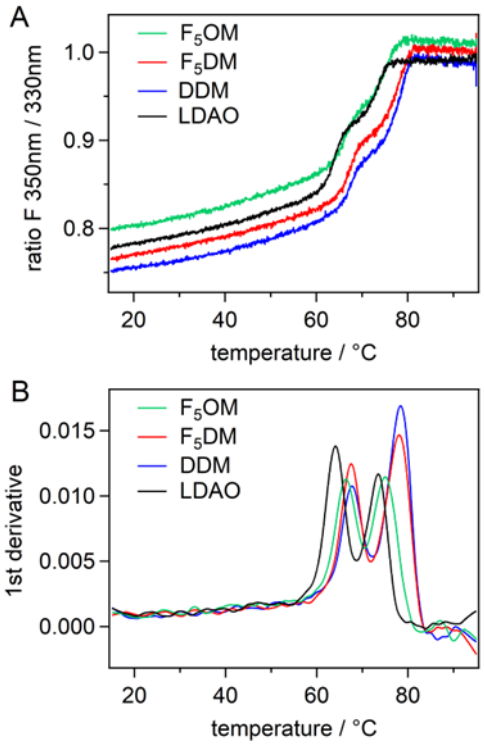


Figure 6. Thermal denaturation of FhuA by differential scanning fluorimetry. (A) Ratio of the fluorescence emitted at 350 and 330 nm, and (B) derivative (bottom panel) for FhuA at 0.04 mg mL^{-1}, incubated in the presence of F_5OM at CMC+2mM (green), F_5DM at CMC+2mM (red), DDM at CMC+0.2mM (blue), LDAO at CMC+2 mM (black).

Table 2. Melting temperatures of FhuA and bR

Protein type	Detergent	Concentration (mM)		T_m (°C)		T_{agg} (°C)
		Detergent	Micelle	T_{m1}	T_{m2}	
FhuA	LDAO	1.20, 3.00	0.2, 2.0	64	73	72
	DDM	0.37, 2.17	0.2, 2.0	68	79	73
	F_5OM	3.00, 4.80	0.2, 2.0	66	75	70
	F_5DM	0.60, 2.40	0.2, 2.0	68	78	73
bR	OTG	9.2, 11.0	0.2, 2.0	54		43

	DDM	0.37, 2.17	0.2, 2.0	60	54
	F_5OM	3.00, 4.80	0.2, 2.0	59	50
	F_5DM	0.60, 2.40	0.2, 2.0	58	55

T_{m1}, T_{m2}, T_m: melting temperatures measured by differential scanning fluorimetry for the first and second transition of FhuA, and the transition for bR, T_{agg}: onset temperature for aggregation from light back reflexion. The precision on T_{m1} is estimated at 1° C, that for T_{m2} and T_m, which are above T_{agg}, at 2° C. The precision on T_{agg} is 2°C. Micelle concentrations (*i.e.* above the CMC concentrations) were calculated considering CMC-values of 1, 0.17, 2.8, and 0.4 mM for LDAO, DDM, F_5OM, and F_5DM, respectively

Homogeneity and stability of bR over time. The retinal molecule bound to bR, whose visible absorption spectrum is very sensitive to its local environment, is a convenient reporter of the state of the protein.[32] Figure 7 reports bR absorption spectra after detergent exchange, over time, in DDM, F_5OM and F_5DM. Pink monomeric bR in DDM displays a λ_{max} = 550 nm. In F_5OM or F_5DM, just after detergent exchange, the λ_{max} ~ 595 nm is compatible with the observed bR blue color, and reflects a monomeric state, as observed previously in various fluorinated surfactants.[35] After two days incubation, λ_{max} shifts to ~ 575 nm (close to the λ_{max} of native bR), and remains unchanged for one year; the absence of λ_{max} = 390 nm, reporter of free retinal, reflects the absence of protein denaturation; over time, the spectra show scattering, witness of progressive but very minor aggregation. These three observations suggest clustering of monomeric bR into larger, native-like oligomers. Thus, the protein is extremely stable as regards its conformation, but its colloidal stability is not as good as that in DDM. When comparing with the previous fluorinated compounds of the maltose series, some differences can be noted: 1- in F_2UDM and F_4NM, bR was blue (λ_{max} ~ 610 nm) and remained so unless it denatured; 2- in F_2UDM, bR was not stable, denatured and aggregated ; 3- in F_6OM, bR was not soluble and aggregated during surfactant exchange.[22] Thus, both F_5OM and F_5DM appear more solubilizing than F_6OM, more stabilizing than F_2UDM and providing a more native environment than F_4NM. Thus, an optimized F/H ratio has been found in those two compounds, providing solubility, stability and close-to-native environment in biochemistry.

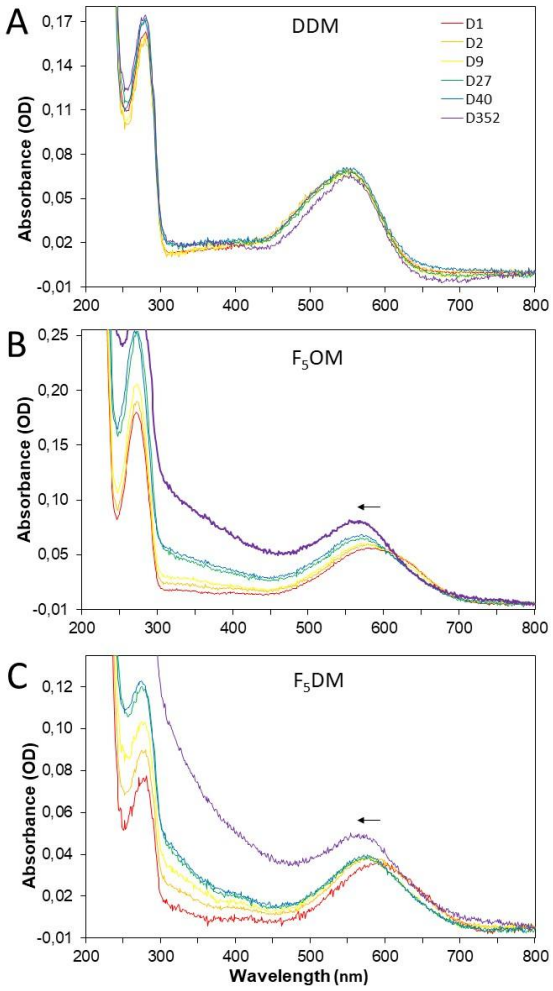


Figure 7. Spectral time course of bR collected from the gradients in (**A**) DDM, (**B**) F_5OM and (**C**) F_5OM. Samples were incubated at 4°C in the dark and UV-visible spectra were recorded at the indicated time (given in days, D). Day 1 curve is displayed in red, day 2 in orange, day 9 in yellow, day 27 in green, day 40 in cyan and day 357 in violet. The arrow indicates the evolution of λ_{max} with time.

Specific activity of BmrA and SpNOX

We investigated the enzymatic stability of two MPs, SpNOX, a *Streptococcus pneumoniae* protein analog to the eukaryotic NADPH oxidase[24] and BmrA, a transporter of multiple drugs with the driving force of ATP hydrolysis.[23]The activity results following detergent exchange are displayed on Figure S6. The specific activity of BmrA and SpNOX is partially preserved, and in the same range for F_5OM, F_5DM, and F_6OM.

Conclusion

We have designed two maltose-based fluorinated surfactants, F_5OM and F_5DM, whose hydrophobic tails are made up of linear fluoroalkyl chains. Formation of micelles in water occurred as governed by the length of the hydrophobic chain. F_5OM and F_5DM self-assembled into rod-like micelles, with hydrodynamic diameters and aggregation numbers that increased with chain length. The potencies of the new FSs to act as detergents was first demonstrated using synthetic POPC lipid vesicles and were further confirmed through the extraction of MPs from *E. coli* membranes. Both F_5OM and F_5DM showed detergency with more solubilizing activity than the commercial fluorinated compound F_6OM at all concentrations and even better protein-extraction efficiency than DDM at low concentrations. F_5DM consistently exhibited better solubilizing properties than F_5OM, towards both lipid vesicles and MPs. The detergency of the two derivatives exceeded by far that of the fluorinated DigluM derivatives F_4H_2-, F_6H_2- and F_8H_2DigluM. This suggests that the linear maltoside polar head, likely owing to its small size, may promote detergency as compared with the bulky branched diglucose polar head. BR and FhuA, representatives of α-helical and ß-barrel proteins, showed remarkable thermal and, for bR, also functional stability, similar to DDM, when transferred into both F_5OM and F_5DM. These surfactants appear, for bR, better than the commercial F_6OM in which the protein aggregated more stabilizing than F_2UDM and provided a more native environment than F_4NM. This indicates that an optimized F/H ratio has been identified in those two compounds, providing solubility, stability, and a close-to-native environment for bR. The enzymatic activities of BmrA and SpNox, were by contrast rather limited when compared to DDM, and similar for F_5OM, F_5H_5OM and F_6OM. Taken together, these findings support the usefulness of this novel series of fluorinated maltoside detergents as promising molecular tools for extracting, stabilizing, and handling MPs.

ASSOCIATED CONTENT

Supporting Information

The supporting information is available free of charge on the ACS Publication website at DOI: #

ITC, ^{19}F NMR and surface tension data curves of F_5OM; Analysis of sedimentation velocity experiments; Small Angle X-Ray Scattering complementary data of F_5OM and F_5DM including concentration dependence analysis and cylinder shape fitting; Thermal denaturation of bR by differential scanning fluorimetry; Material and Methods for BmrA and SpNox production and SpNox and BmrA activity assays; SpNox and BmrA activity data in F_6OM, F_5OM and F_5DM;

^1H and ^{13}C NMR spectra and mass spectrometry data of compounds **2a** and **2b**; ^1H, 19F and ^{13}C NMR spectra and mass spectrometry data of compounds **3a**, **3b**, **4a** (F_5OM) and **4b** (F_5DM).

Acknowledgment.

This work was supported by the Agence Nationale de la Recherche (ANR) through grants no. ANR-16-CE92-0001, by the Deutsche Forschungsgemeinschaft (DFG) through grant no. KE 1478/7 1, and by the Deutsche Akademische Austauschdienst (DAAD) with a grant to K.K.O. We acknowledge the financial support of the European Regional Development Fund, the French Government, the “Région Provence Alpes Côte d'Azur”, the “Département de Vaucluse” and the “Communauté d’agglomération Grand Avignon” for access to the NMR platform (CPER 3A). This work used the platforms of the Grenoble Instruct-ERIC center (ISBG; UMS 3518 CNRS-CEA-UGA-EMBL) within the Grenoble Partnership for Structural Biology (PSB), supported by FRISBI (ANR-10-INBS-05-02) and GRAL, financed within the University Grenoble Alpes graduate school (Ecoles Universitaires de Recherche) CBH-EUR-GS (ANR-17-EURE-0003). IBS acknowledges integration into the Interdisciplinary Research

Institute of Grenoble (IRIG, CEA) We thank Martha Brennich (ESRF) for help in SAXS data acquisition and Marine Soulié (IBMM) for carefully checking NMR data. Emmi Mikkola (UGA) participated to the biochemical evaluation during her master internships at IBS. This work benefited from the use of the SasView application, originally developed under NSF Award DMR- 0520547. SasView also contains code developed with funding from the EU Horizon 2020 programme under the SINE2020 project Grant No 654000.

References

1. Overington, J. P.; Al-Lazikani, B.; Hopkins, A. L., How many drug targets are there? *Nature Reviews Drug Discovery* **2006,** *5* (12), 993-996.

2. Arachea, B. T.; Sun, Z.; Potente, N.; Malik, R.; Isailovic, D.; Viola, R. E., Detergent selection for enhanced extraction of membrane proteins. *Protein expression and purification* **2012,** *86* (1), 12-20.

3. Morandat, S.; El Kirat, K., Solubilization of supported lipid membranes by octyl glucoside observed by time-lapse atomic force microscopy. *Colloids and Surfaces B: Biointerfaces* **2007,** *55* (2), 179-184.

4. Vacklin, H. P.; Tiberg, F.; Thomas, R. K., Formation of supported phospholipid bilayers via co-adsorption with β-d-dodecyl maltoside. *Biochimica et Biophysica Acta (BBA) - Biomembranes* **2005,** *1668* (1), 17-24.

5. Ai, X.; Caffrey, M., Membrane Protein Crystallization in Lipidic Mesophases: Detergent Effects. *Biophysical Journal* **2000,** *79* (1), 394-405.

6. Rouse, S. L.; Marcoux, J.; Robinson, C. V.; Sansom, M. S. P., Dodecyl maltoside protects membrane proteins in vacuo. *Biophysical Journal* **2013,** *105* (3), 648-656.

7. Lebaupain, F.; Salvay, A. G.; Olivier, B.; Durand, G.; Fabiano, A.-S.; Michel, N.; Popot, J.-L.; Ebel, C.; Breyton, C.; Pucci, B., Lactobionamide Surfactants with Hydrogenated, Perfluorinated or Hemifluorinated Tails: Physical-Chemical and Biochemical Characterization. *Langmuir* **2006,** *22* (21), 8881-8890.

8. Fayolle, D.; Berthet, N.; Doumeche, B.; Renaudet, O.; Strazewski, P.; Fiore, M., Towards the preparation of synthetic outer membrane vesicle models with micromolar affinity to wheat germ agglutinin using a dialkyl thioglycoside. *Beilstein Journal of Organic Chemistry* **2019,** *15*, 937-946.

9. Asada, A.; Sonoyama, M., Solubilization and Structural Stability of Bacteriorhodopsin with a Mild Nonionic Detergent, n-Octyl-β-thioglucoside. *Bioscience, Biotechnology, and Biochemistry* **2011,** *75* (2), 376-378.

10. Guillet, P.; Mahler, F.; Garnier, K.; Nyame Mendendy Boussambe, G.; Igonet, S.; Vargas, C.; Ebel, C.; Soulié, M.; Keller, S.; Jawhari, A.; Durand, G., Hydrogenated Diglucose Detergents for Membrane-Protein Extraction and Stabilization. *Langmuir* **2019,** *35* (12), 4287-4295.

11. Dauvergne, J.; Desuzinges, E. M.; Faugier, C.; Igonet, S.; Soulié, M.; Grousson, E.; Cornut, D.; Bonneté, F.; Durand, G.; Dejean, E.; Jawhari, A., Glycosylated Amphiphilic Calixarene-Based Detergent for Functional Stabilization of Native Membrane Proteins. *ChemistrySelect* **2019,** *4* (19), 5535-5539.

12. Breyton, C.; Javed, W.; Vermot, A.; Arnaud, C.-A.; Hajjar, C.; Dupuy, J.; Petit-Hartlein, I.; Le Roy, A.; Martel, A.; Thépaut, M.; Orelle, C.; Jault, J.-M.; Fieschi, F.; Porcar, L.; Ebel, C., Assemblies of lauryl maltose neopentyl glycol (LMNG) and LMNG-solubilized membrane proteins. *Biochimica et Biophysica Acta (BBA) - Biomembranes* **2019,** *1861* (5), 939-957.

13. Cho, K. H.; Husri, M.; Amin, A.; Gotfryd, K.; Lee, H. J.; Go, J.; Kim, J. W.; Loland, C. J.; Guan, L.; Byrne, B.; Chae, P. S., Maltose neopentyl glycol-3 (MNG-3) analogues for membrane protein study. *Analyst* **2015,** *140* (9), 3157-3163.

14. Chae, P. S.; Rasmussen, S. G. F.; Rana, R. R.; Gotfryd, K.; Chandra, R.; Goren, M. A.; Kruse, A. C.; Nurva, S.; Loland, C. J.; Pierre, Y.; Drew, D.; Popot, J.-L.; Picot, D.; Fox, B. G.; Guan, L.; Gether, U.; Byrne, B.; Kobilka, B.; Gellman, S. H., Maltose–neopentyl glycol (MNG) amphiphiles for solubilization, stabilization and crystallization of membrane proteins. *Nature Methods* **2010,** *7*, 1003.

15. Sadtler, V. M.; Giulieri, F.; Krafft, M. P.; Riess, J. G., Micellization and Adsorption of Fluorinated Amphiphiles: Questioning the 1 CF2≈1.5 CH2 Rule. *Chemistry – A European Journal* **1998,** *4* (10), 1952-1956.

16. Krafft, M. P.; Riess, J. G., Highly fluorinated amphiphiles and colloidal systems, and their applications in the biomedical field. A contribution. *Biochimie* **1998,** *80* (5), 489-514.

17. Riess, J. G.; Krafft, M. P., Fluorinated materials for in vivo oxygen transport (blood substitutes), diagnosis and drug delivery. *Biomaterials* **1998,** *19* (16), 1529-1539.

18. Durand, G.; Abla, M.; Ebel, C.; Breyton, C., New Amphiphiles to Handle Membrane Proteins: "Ménage à Trois" Between Chemistry, Physical Chemistry, and Biochemistry. In *Membrane Proteins Production for Structural Analysis*, Mus-Veteau, I., Ed. Springer New York: 2014; pp 205-251.

19. Frotscher, E.; Danielczak, B.; Vargas, C.; Meister, A.; Durand, G.; Keller, S., A Fluorinated Detergent for Membrane-Protein Applications. *Angewandte Chemie International Edition* **2015,** *54* (17), 5069-5073.

20. Boussambe, G. N. M.; Guillet, P.; Mahler, F.; Marconnet, A.; Vargas, C.; Cornut, D.; Soulié, M.; Ebel, C.; Le Roy, A.; Jawhari, A.; Bonneté, F.; Keller, S.; Durand, G., Fluorinated diglucose detergents for membrane-protein extraction. *Methods* **2018,** *147*, 84-94.

21. Polidori, A.; Presset, M.; Lebaupain, F.; Ameduri, B.; Popot, J.-L.; Breyton, C.; Pucci, B., Fluorinated and hemifluorinated surfactants derived from maltose: Synthesis and application to handling membrane proteins in aqueous solution. *Bioorganic & Medicinal Chemistry Letters* **2006,** *16* (22), 5827-5831.

22. Polidori, A.; Raynal, S.; Barret, L.-A.; Dahani, M.; Barrot-Ivolot, C.; Jungas, C.; Frotscher, E.; Keller, S.; Ebel, C.; Breyton, C.; Bonnete, F., Sparingly fluorinated maltoside-based surfactants for membrane-protein stabilization. *New Journal of Chemistry* **2016,** *40* (6), 5364-5378.

23. Ravaud, S.; Do Cao, M.-A.; Jidenko, M.; Ebel, C.; Le Maire, M.; Jault, J.-M.; Di Pietro, A.; Haser, R.; Aghajari, N., The ABC transporter BmrA from Bacillus subtilis is a functional dimer when in a detergent-solubilized state. *Biochemical Journal* **2006,** *395* (2), 345-353.

24. Hajjar, C.; Cherrier, M. V.; Dias Mirandela, G.; Petit-Hartlein, I.; Stasia, M. J.; Fontecilla-Camps, J. C.; Fieschi, F.; Dupuy, J., The NOX Family of Proteins Is Also Present in Bacteria. *mBio* **2017,** *8* (6), e01487-17.

25. Braun, V., FhuA (TonA), the career of a protein. *Journal of Bacteriology* **2009,** *191* (11), 3431-6.

26. Pebay-Peyroula, E.; Rummel, G.; Rosenbusch, J. P.; Landau, E. M., X-ray Structure of Bacteriorhodopsin at 2.5 Angstroms from Microcrystals Grown in Lipidic Cubic Phases. *Science* **1997,** *277* (5332), 1676-1681.

27. Schuck, P., Size-distribution analysis of macromolecules by sedimentation velocity ultracentrifugation and lamm equation modeling. *Biophysical Journal* **2000,** *78*, 1606-1619.

28. Brautigam, C. A., Chapter Five - Calculations and Publication-Quality Illustrations for Analytical Ultracentrifugation Data. In *Methods in Enzymology*, Cole, J. L., Ed. Academic Press: 2015; Vol. 562, pp 109-133.

29. Salvay, A. G.; Ebel, C., Analytical Ultracentrifuge for the Characterization of Detergent in Solution. In *Analytical Ultracentrifugation VIII.* , Wandrey, C.; Cölfen, H., Eds. Springer: Berlin, Heidelberg, 2006; Vol. 131.

30. Pernot, P.; Round, A.; Barrett, R.; De Maria Antolinos, A.; Gobbo, A.; Gordon, E.; Huet, J.; Kieffer, J.; Lentini, M.; Mattenet, M.; Morawe, C.; Mueller-Dieckmann, C.; Ohlsson, S.; Schmid, W.; Surr, J.; Theveneau, P.; Zerrad, L.; McSweeney, S., Upgraded ESRF BM29 beamline for SAXS on macromolecules in solution. *Journal of Synchrotron Radiation* **2013,** *20* (4), 660-664.

31. Petoukhov, M. V.; Franke, D.; Shkumatov, A. V.; Tria, G.; Kikhney, A. G.; Gajda, M.; Gorba, C.; Mertens, H. D. T.; Konarev, P. V.; Svergun, D. I., New developments in the ATSAS program package for small-angle scattering data analysis. *Journal of Applied Crystallography* **2012,** *45* (2), 342-350.

32. Breyton, C.; Gabel, F.; Abla, M.; Pierre, Y.; Lebaupain, F.; Durand, G.; Popot, J.-L.; Ebel, C.; Pucci, B., Micellar and biochemical properties of (hemi)fluorinated surfactants are controlled by the size of the polar head. *Biophysical Journal* **2009,** *97*, 1-10.

33. Ciastek, S.; Szymańska, K.; Kaszyński, P.; Jasiński, M.; Pociecha, D., Smectic behaviour of methyl 4-alkoxybenzoates with a partially fluorinated alkyl chain. *Liquid Crystals* **2018,** *45* (1), 11-21.

34. Ren, B.; Wang, M.; Liu, J.; Ge, J.; Zhang, X.; Dong, H., Zemplén transesterification: a name reaction that has misled us for 90 years. *Green Chemistry* **2015,** *17* (3), 1390-1394.

35. Tanford, C., Thermodynamics of Micelle Formation: Prediction of Micelle Size and Size Distribution. *Proceedings of the National Academy of Sciences* **1974,** *71* (5), 1811-1815.

36. Broecker, J.; Keller, S., Impact of urea on detergent micelle properties. *Langmuir* **2013,** *29*, 8502–8510.

37. Sadtler, V. M.; Giulieri, M. P.; M.P., K.; Riess, J. G., Micellization and Adsorption of Fluorinated Amphiphiles: Questioning the 1CF2 ~1.5CH2 Rule. *Chem. Eur. J.* **1998,** *4*, 1952-1957.

38. Al-Soufi, W.; Piñeiro, L.; Novo, M., A model for monomer and micellar concentrations in surfactant solutions: application to conductivity, NMR, diffusion, and surface tension data. *J. Coll. Interface Sci.* **2012,** *370* (1), 102-110.

39. Svergun, D. I.; Koch, M. H. J., Small-angle scattering studies of biological macromolecules in solution. *Reports on Progress in Physics* **2003,** *66* (10), 1735-1782.

40. Lipfert, J.; Columbus, L.; Chu, V. B.; Lesley, S. A.; Doniach, S., Size and Shape of Detergent Micelles Determined by Small-Angle X-ray Scattering. *The Journal of Physical Chemistry B* **2007,** *111* (43), 12427-12438.

41. Oliver, R. C.; Pingali, S. V.; Urban, V. S., Designing Mixed Detergent Micelles for Uniform Neutron Contrast. *The Journal of Physical Chemistry Letters* **2017,** *8* (20), 5041-5046.

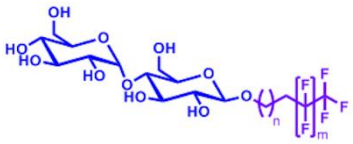
42. Oliver, R. C.; Lipfert, J.; Fox, D. A.; Lo, R. H.; Doniach, S.; Columbus, L., Dependence of micelle size and shape on detergent alkyl chain length and head group. *PloS one* **2013,** *8* (5), e62488.

43. Ferguson, A. D.; Hofmann, E.; Coulton, J. W.; Diederichs, K.; Welte, W., Siderophore-Mediated Iron Transport: Crystal Structure of FhuA with Bound Lipopolysaccharide. *Science* **1998,** *282* (5397), 2215-2220.

44. Wang, J.; Link, S.; Heyes, C. D.; El-Sayed, M. A., Comparison of the dynamics of the primary events of bacteriorhodopsin in its trimeric and monomeric states. *Biophysical Journal* **2002,** *83* (3), 1557-1566.

45. Flayhan, A.; Wien, F.; Paternostre, M.; Boulanger, P.; Breyton, C., New insights into pb5, the receptor binding protein of bacteriophage T5, and its interaction with its Escherichia coli receptor FhuA. *Biochimie* **2012,** *94*, 1982-1989.

Table of Graphical Content



	n	m	Solubilization	Extraction	Stabilization
F_6OM	1	5	😐	😐	☹
F_5OM	2	4	☺	☺	☺
F_5DM	4	4	☺	☺	☺